24th INTERNATIONAL CONGRESS ON SOUND AND VIBRATION
23–27 July 2017, London

ICSV24
23-27JULY 2017
LONDON CALLING

APPLICATION OF HIGHER ORDER SPECTRA FOR THE FATIGUE LOAD CHARACTERISATION OF NON-GAUSSIAN RANDOM VIBRATION SIGNALS

Arthur Hammer* and Peter Wolfsteiner

University of Applied Sciences Munich, Department 03, Munich, Germany
**email: arthur.hammer@outlook.de*

Fatigue assessment of vibrating structures is usually made in time domain, where a well-established set of tools to calculate load spectra is available (e.g. Rainflow Counting). However, when analysing fatigue under random excitations on linear vibration systems, frequency domain methods were preferred, because they offer precise definitions of random signals and also great computation advantages. Currently available methods of this type are based on the signals power spectral density (PSD) and corresponding methods for the estimation of load spectra (e.g. Dirlik method). The PSD is the second order spectrum and therefore only describes Gaussian distributed random signals adequately. Applying PSD-based methods for non-Gaussian random signals, which often occur in real world applications, can cause significant errors in load spectra estimations. A commonly used parameter to assess the deviation of a random signal's probability distribution compared to a Gaussian distribution is the value of kurtosis. Hence, methods were developed, which use this kurtosis value to assess and also correct inappropriately estimated load spectra. The presented paper shows that this single kurtosis parameter is insufficient for a precise characterisation of non-Gaussian vibration signals. This can be achieved by the use of higher order spectra, which allow a characterisation of these deviations from a Gaussian distribution in frequency domain. Currently available estimation techniques for these higher order spectra are limited to quite short time signals. Though, fatigue analysis of random vibrations is often based on long measured time signals (e.g. up to 10^9 samples). Therefore this paper further presents an efficient and robust method for calculating higher order spectra of very long time signals as a whole. This technique can replace the usually applied error-prone averaging methods that are based on the analysis of short time signals.

Keywords: non-Gaussian random vibrations, frequency domain fatigue, higher order spectra

1. Introduction

Mechanical structures are often subjected to random service load vibrations throughout a long period of time, leading to relevant fatigue loads. Therefore adequate assessment methods are needed. Usually this is done in time domain, where vibrating structures were modelled using Finite Element Methods (FEM) or Multibody Systems (MBS) and subjected to measured or simulated vibration loads $x(t)$. The resulting stress responses $y(t)$ can then be analysed by fatigue cycle counting methods, e.g. the widely accepted Rainflow Counting (RFC) [1] in order to determine load spectra $s^{RFC}(N)$. They concentrate fatigue cycle amplitudes over a cumulated number of cycles. Finally damage accumulation theorems, e.g. Palmgren Miner (PM) [2], enable an assessment of the structure's state of fatigue, e.g. expressed as equivalent (constant) stress amplitude s_{eq} with the corresponding number N_{eq} of stress cycles [3] (see Fig. 1 a). When analysing fatigue under random vibration loads, time domain based fatigue assessment methods can get computationally inapplicable,

since the random vibration loads must be quite long in order to capture the signal's statistical properties adequately. Additionally, with an increasing complexity of the vibration model (e.g. in FEM), the simulation efforts to evaluate the structure's stress response even get worse. Therefore, very efficient frequency domain techniques were developed (see [4-6]) that offer much faster simulations of linear vibration structures and also enable an adequate definition of random vibration loads in terms of power spectral densities (PSD). Once the PSD of the structure's stress response $S_{yy}(f)$ is computed, the load spectra $s^{DK}(N)$ can be estimated using the Dirlik method (DK) [7] or others [8]. Fig. 1 b schematically shows an overview of a specific frequency based fatigue analysis procedure on random vibration loads using the DK estimator.

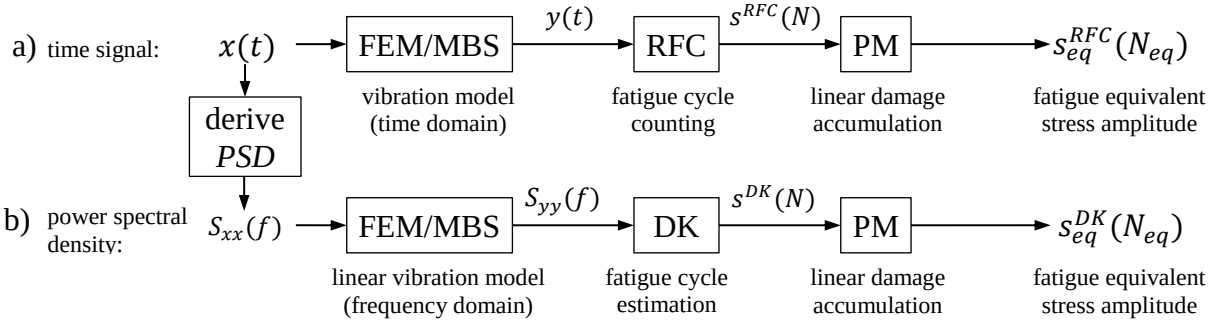

Figure 1: Concept of fatigue assessment of random vibration loads in a) time or b) frequency domain

These very efficient PSD-based simulation methods work very well if the random vibration load is Gaussian distributed (e.g. [8]). Deviations from the Gaussian distribution may cause severe deviations in the estimated loads (e.g. [9-11]). As engineering problems are often related to non-Gaussian random vibrations, considerable research has been done to solve this issue (e.g. [10, 12, 13]). The proposed solutions are mainly based on the assumption, that the deviation to a Gaussian distribution is a single property valid for the entire frequency range of the signal. A typically used concept for describing this deviation is the kurtosis value β, which is based on the second and fourth order moment of the probability distribution (see Eq. (1)). [14] shows, that the deviation from a Gaussian distribution has to be understood as a property depending on the frequency of the random signal. This paper now presents a conclusive analysis tool for this issue based on the application of higher order spectra. They allow a well-founded insight into the distribution of higher order statistical moments in the frequency range of the signal. To demonstrate the capacity of these tools, an example with two different random signals having identical PSD and probability distribution (PD) (therefore also identical kurtosis) is presented. Despite these similar statistical properties, the signals will have a totally different fatigue impact on linear vibration systems.

Therefore, this paper presents some basic facts about the analysis of random vibration signals in section 2. It shortly introduces higher order spectra, their importance in characterising non-Gaussian random vibration signals and the way they were usually computed (with a strong limitation to short time signals). It then introduces an efficient method to compute higher order spectra of very long vibration signals as a whole. In section 3, this paper defines an example of two different non-Gaussian random vibration loads having equal PSD and probability distribution. By applying the commonly accepted Fatigue Damage Spectrum (FDS, see [15]) it is shown, that these signals have a completely different impact on the fatigue of a vibration system.

2. Analysis of non-Gaussian random signals

2.1 Second order spectral analysis

For the analysis of a random vibration signal $x(t)$ with zero mean ($\bar{x} = 0$) and a length of time T, there are some major quantities of importance. The most common ones are variance σ^2, skewness γ and kurtosis β. They can be derived from the central moments m_i of i-th order [4].

$$\sigma^2 = m_2, \quad \gamma = m_3/m_2^{3/2}, \quad \beta = m_4/m_2^{4/2}, \quad \text{with: } m_i = \lim_{T\to\infty} \frac{1}{T} \int_0^T x(t)^i \, dt \tag{1}$$

In analogy to Eq. (1), where the variance is computed by integration in time domain, it can also be computed by integration in frequency domain [16], where $S_{xx}(f)$ is the PSD of signal $x(t)$.

$$\sigma^2 = m_2 = \int_{-\infty}^{\infty} S_{xx}(f) \, df \tag{2}$$

Spectral analysis offers different methods for the derivation of PSDs. The indirect method is based on the autocorrelation function $R_{xx}(\tau)$ of $x(t)$ (Wiener Khinchin Theorem [16], where j denotes the imaginary unit and τ the time lag).

$$S_{xx}(f) = \int_{-\infty}^{\infty} R_{xx}(\tau) \, e^{-2j\pi f\tau} \, d\tau, \quad \text{with: } R_{xx}(\tau) = \lim_{T\to\infty} \frac{1}{T} \int_0^T x(t)x(t+\tau) \, dt \tag{3}$$

The direct method is based on the Periodogram [16] ($X(f)$ is the Fourier Transformation of $x(t)$, * denotes the conjugate complex).

$$S_{xx}(f) = \lim_{T\to\infty} \frac{1}{T} \, X(f) \, X^*(f), \quad \text{with: } X(f) = \lim_{T\to\infty} \int_0^T x(t) \, e^{-2j\pi ft} \, dt \tag{4}$$

There are more common methods for PSD estimation, like the Bartlett or the Welch method, which are modified versions of the Periodogram in a way of using time sample overlaps or averaging techniques. A special feature of the central moments appears, when the vibration signal $x(t)$ is Gaussian distributed and of zero mean: the higher order central moments are either zero (for odd orders) or just defined by the variance σ^2 (for even orders) [17, 18].

$$\begin{array}{lllll} m_0 = 1 & m_2 = \sigma^2 & m_4 = 3\sigma^4 & m_6 = 15\sigma^6 & m_8 = 105\sigma^8 \quad ... \\ m_1 = \bar{x} & m_3 = 0 & m_5 = 0 & m_7 = 0 & m_9 = 0 \quad ... \end{array} \tag{5}$$

This means, that if $x(t)$ is Gaussian distributed and of zero mean, there is no further information in higher order central moments; skewness and kurtosis turn out to be $\gamma = 0$ and $\beta = 3$. However, if the vibration signal is non-Gaussian, higher order moments contain all the information about the actual probability distribution. This is probably the reason why the kurtosis β has become a commonly used indicator for the deviation from a Gaussian distribution. Since β is just a single parameter, it summarizes the 4th order non-Gaussian properties of a random signal for its entire frequency range, but it does not contain any further information about the frequency distribution of m_4. For the 2nd moment m_2 this information is already available from Eq. (2). The solution of this integral of a limited frequency interval Δf might be understood as the distribution of the 2nd moment in the frequency range f of signal $x(t)$.

$$m_2(f, \Delta f) = \int_f^{f+\Delta f} S_{xx}(f) \, df \tag{6}$$

This 2nd moment also corresponds to the variance σ_n^2 of a band pass filtered signal $x(t, n)$ within the frequency interval n from $(n-1)\Delta f$ to $n\Delta f$ (see [16]). In analogy to this 2nd order moment, higher order spectra give equal relations for the distribution of higher order moments in frequency domain. As this information is indispensable for a proper understanding of a non-Gaussian signal, the next section offers the necessary tools from the area of higher order spectral analysis.

2.2 Higher order spectral analysis

In analogy to the 2nd order moment, higher order spectra give equal relations for the distribution of higher order moments in frequency domain. For example, the distribution of the 4th order moment in frequency domain, which relates with the kurtosis, is represented by the 4th order spectrum (also known as trispectrum). In general, higher order spectra can be calculated in an equal manner compared to the computation of the PSD. In analogy to the indirect method, the i-th order spectrum S_i^x of the vibration signal $x(t)$ can be computed by the Fourier Transformation of the i-th order autocorrelation function [19]

$$S_i^x(f_1, \cdots, f_{i-1}) = \int_{-\infty}^{\infty} \cdots \int_{-\infty}^{\infty} R_i^x(\tau_1, \cdots, \tau_{i-1}) \, e^{-2j\pi(f_1\tau_1, \cdots, f_{i-1}\tau_{i-1})} \, d\tau_1 \cdots d\tau_{i-1}, \tag{7}$$

$$R_i^x(\tau_1, \cdots, \tau_{i-1}) = \lim_{T\to\infty} \frac{1}{T} \int_0^T x(t)x(t+\tau_1) \cdots x(t+\tau_{i-1}) \, dt. \tag{8}$$

In analogy to the direct method, there is a similar computation method to compute the i-th order spectrum by Polyperiodograms [19].

$$S_i^x(f_1,\cdots,f_{i-1}) = \lim_{T\to\infty}\frac{1}{T}X(f_1)\cdots X(f_{i-1})X^*(f_1+\cdots+f_{i-1}) \tag{9}$$

Both methods, Eqs. (7) and (9), appear as Eqs. (3) and (4) for $i = 2$. This points out, that the PSD is the 2nd order spectrum, containing the information of the 2nd order central moment in frequency domain or the variance, respectively. In a similar way as higher order central moments contain no further information about the statistical properties of a Gaussian distributed random vibration signal with zero mean, higher order spectra also contain only trivial information about the Gaussian distributed vibration signal in frequency domain. This is because one can get to the central moments of a Gaussian distributed random vibration signal (see Eq. (5)) by integration of higher order spectra in frequency domain [17,19].

$$m_i = \int_{-\infty}^{\infty}\cdots\int_{-\infty}^{\infty} S_i^x(f_1,\cdots,f_{i-1})\,df_1\cdots df_{i-1} \tag{10}$$

Nevertheless, if the random vibration signal is non-Gaussian, higher order spectra contain the information about non-Gaussian properties of the random vibration signal in frequency domain.

2.3 Efficient computation method for higher order spectra and long time signals

Applying Eq. (7) or (9) on even a short time vibration signal (e.g. with 10^4 data points), computation efforts turn out to be infeasible. This is because of the multidimensional character of higher order spectra, which means that multidimensional Fourier Transforms (see Eq. (7)) or numerically costly frequency combinatorics (see Eq. (9)) were needed. Furthermore, because of its multidimensional appearance, higher order spectra are also challenging in the amount of data, because already a trispectrum ($i = 4$) is represented by a three dimensional array with $(10^4)^3$ data points. This is why higher order spectra algorithms are usually just applied on very short time signals if necessary together with error-prone averaging techniques [20, 21]. Nevertheless, once the higher order spectra are calculated, the amount of data may be strongly reduced by piecewise integration in frequency bands n to a certain reasonable resolution (corresponding to Eq. (6)).

$$m_i(n_1,\cdots,n_{i-1}) = \int_{n_1}\cdots\int_{n_{i-1}} S_i^x(f_1,\cdots,f_{i-1})\,df_1\cdots df_{i-1}, \quad \text{with:} \quad -\infty < n < \infty \tag{11}$$

This underscores the need of a more efficient method, which is able to calculate the reduced higher order spectra without the need of calculating the higher order spectra in its full resolution first. This can be achieved by taking Eq. (7) and (8) and reformulating them. After some substitutions for $t+\tau$ and the use of the Fourier Transformation one can find the following expression.

$$S_i^x(f_1,\dots f_{i-1}) = \lim_{T\to\infty}\int_0^T x(t)\,X(f_1)e^{2j\pi f_1 t}\cdots X(f_{i-1})e^{2j\pi f_{i-1}t}\,dt \tag{12}$$

This equation may now be substituted into Eq. (10) for reformulation until getting the following.

$$m_i = \lim_{T\to\infty}\int_0^T x(t)\lim_{f_1\to\infty}\int_{-f_1}^{f_1} X(f_1)e^{2j\pi f_1 t}\,df_1\cdots\lim_{f_{i-1}\to\infty}\int_{-f_{i-1}}^{f_{i-1}} X(f_{i-1})e^{2j\pi f_{i-1}t}\,df_{i-1}dt \tag{13}$$

If the integrations of Eq. (13) were evaluated for the whole range of frequencies, this expression turns out to be the equation of the i-th order central moment again (see Eq. (1)). Now it is possible to use the piecewise integration, as mentioned in Eq. (11); Eq. (13) becomes the following.

$$m_i(n_1,\dots,n_{i-1}) = \lim_{T\to\infty}\int_0^T x(t)\int_{n_1} X(f_1)e^{2j\pi f_1 t}df_1\cdots\int_{n_{i-1}} X(f_{i-1})e^{2j\pi f_{i-1}t}df_{i-1}\,dt \tag{14}$$

The piecewise integration turns out to be inverse Fourier Transformations over a specific range of two-sided frequencies. In this manner, every piecewise integration over the frequency works like a bandwidth filter for interval n, which gives the filtered complex vibration signal:

$$x(t,n) = \int_n X(f)e^{2j\pi ft}\,df \tag{15}$$

The reduced higher order spectra may then be evaluated by the following alternative equation.

$$m_i(n_1, \dots, n_{i-1}) = \lim_{T\to\infty} \int_0^T x(t)\ x(t, n_1)\ \cdots\ x(t, n_{i-1})\ dt \qquad (16)$$

This equation enables a computation of the reduced higher order spectra without the numerically costly evaluation of the higher order spectra in its full resolution (see. Eqs. (7) and (9)). By the use of Eq. (16), it is possible to switch from the single value of a certain central moment (see Eq. (1)) to the corresponding higher order spectra in a reasonable resolution or even in its full resolution (see Eqs. (7) or (9)). Since filtering can be performed numerically very efficiently based on fast Fourier Transform algorithms, this method may be applied to very long vibration signals (e.g. 10^9) as they usually appear in fatigue applications or, applied to short time signals, even in real time. A simple performance test on an ordinary computer system shows the huge computation advantage. Deriving the reduced trispectra with 24 two-sided frequency bands n of a certain random vibration signal with 10^4 data points under the use of Eq. (9) took approximately 10 h. The same trispectra was evaluated with the proposed method from Eq. (16) in about 1 s. So far filter based spectra estimation methods have only been found for the determination of PSDs (e.g. [16]). The presented method widens the filter based spectra estimation techniques to higher orders.

In section 3, the presented method will be used to evaluate the 4th order spectrum of two different, specifically designed non-Gaussian random vibration signals with equal PSD and distribution. This will demonstrate kurtosis related properties of the signals in certain frequency bands and will also explain their different impact on the fatigue load of a vibration system.

3. Fatigue assessment of non-Gaussian random signals

3.1 Generation of different non-Gaussian random vibration signals with same PSD

Depending on the field of application, there are different ways of generating non-Gaussian random vibration signals; [22] gives an overview. The general intention of the presented paper is to demonstrate that different non-Gaussian random signals (here e.g. $x_{ng1}(t)$ and $x_{ng2}(t)$) each with a different fatigue impact on a vibration system can have identical PSD and distribution. For the generation of these signals a technique is used starting from a random Gaussian signal $x_g(t)$ (here with a constant PSD from 0 to 600Hz, a standard deviation $\sigma = 1\,mm$ and a sample number of $1.2 \cdot 10^6$) multiplied with a slowly changing non-Gaussian random signal $a(t)$: $x_{ng}(t) = a(t) \cdot x_g(t)$ [16]. The resulting signal $x_{ng}(t)$ is again scaled to $\sigma = 1\,mm$ and is assumed to be stationary. $x_{ng}(t)$ may then be expressed in frequency domain with a complex set of $6 \cdot 10^5$ Fourier coefficients $X_{ng}(f)$ (one-sided), represented as magnitudes $|X_{ng}(f)|$ and phases $\varphi_{ng}(f)$. The different signals $x_{ng1}(t)$ and $x_{ng2}(t)$ are now generated by replacing these phase angles $\varphi_{ng}(f)$ by new, synthetically generated, equally distributed phases either in the first (range 1: $0 \le f < 300$Hz, phases $\varphi_{ng1}(f)$, see Fig. 2 in grey) or second (range 2: $300 < f \le 600$Hz, phases $\varphi_{ng2}(f)$, see Fig. 2 in grey) half of the frequency range of $X_{ng}(f)$. Subsequent inverse Fourier Transformations produce the two non-Gaussian random vibration signals $x_{ng1}(t)$ and $x_{ng2}(t)$ (Fig. 3 a and d) in time domain with nearly equal distribution. Since the PSD is real valued and just depending on $|X_{ng}(f)|$, both signals share the same PSD and standard deviation of $\sigma = 1\,mm$. Fig. 2 shows the generation process schematically.

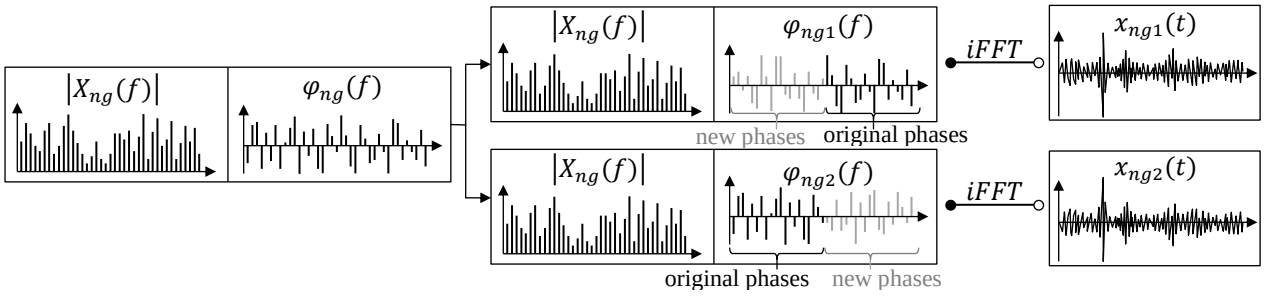

Figure 2: Different non-Gaussian random vibration loads with equal PSD and distribution

Further, the trispectra of $x_{ng1}(t)$ and $x_{ng2}(t)$ were analysed in terms of the 4th order moments $m_{4,ng1}(n_1, n_2, n_3)$ and $m_{4,ng2}(n_1, n_2, n_3)$ corresponding to the method presented in section 2 (see Eq. (16)). Therefore 24 frequency bands (n =-12 ... 12, two-sided corresponding to -600Hz $\leq f \leq$ 600Hz) have been used. Consequently the results consist of 24^3 data points in three dimensions $n_{1,2,3}$. As neither a full introduction to the interpretation of trispectra nor a complete display of these data is impossible in 2D, just some selected data are presented and explained here.

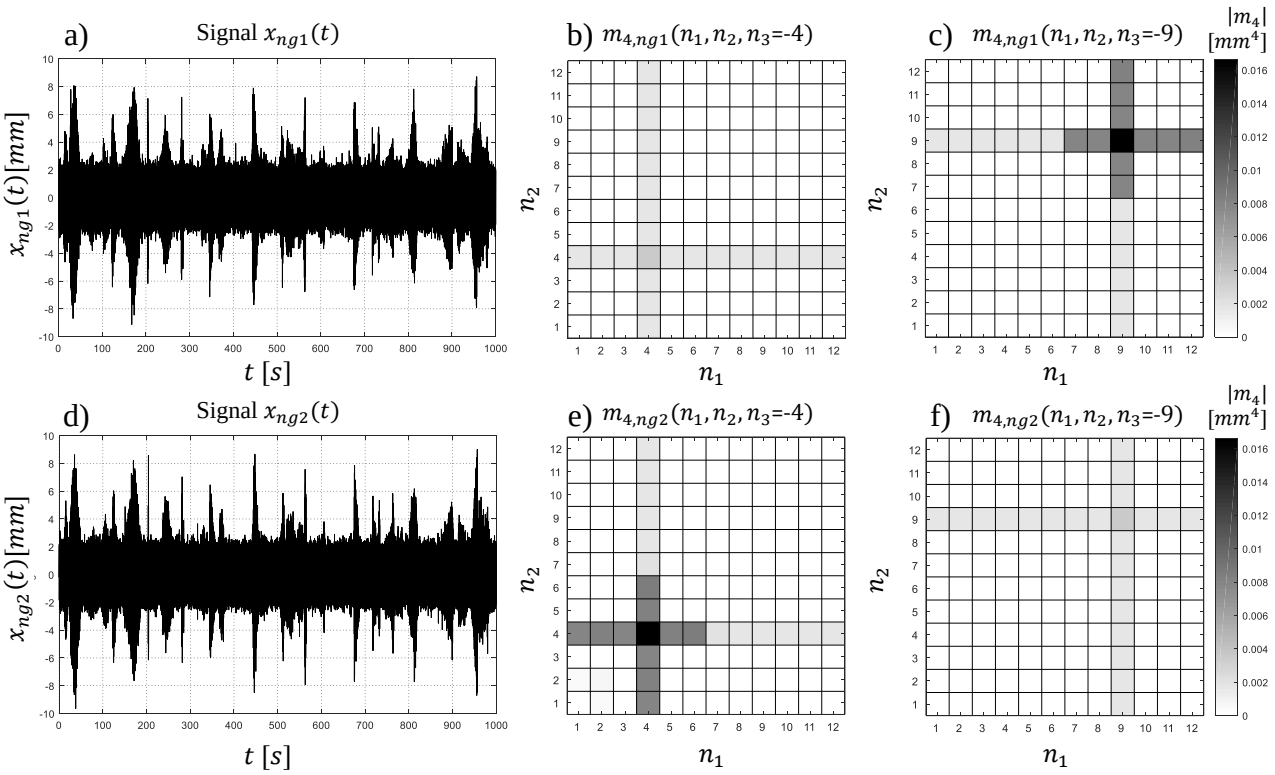

Figure 3: a) Signal $\boldsymbol{x_{ng1}(t)}$ ($\boldsymbol{\beta = 5.7}$), its trispectrum in b) for $\boldsymbol{n_3 = -4}$ and c) for $\boldsymbol{n_3 = -9}$, d) signal $\boldsymbol{x_{ng2}(t)}$ ($\boldsymbol{\beta = 5.7}$), its trispectrum in e) for $\boldsymbol{n_3 = -4}$ and f) for $\boldsymbol{n_3 = -9}$

They show the two signals and cross sections of their trispectra at $n_3 = -4$ and $n_3 = -9$, representative for the first and second half of the negative frequency range, respectively. $n_1$and n_2 were shown for the entire positive frequency range, consisting the first ($1 \leq n \leq 6$) and second ($7 \leq n \leq 12$) half. Comparing $x_{ng1}(t)$ and $x_{ng2}(t)$, the trispectra clearly show different values for m_4 in the first half of the frequency range, where $x_{ng2}(t)$ has kept its non-Gaussianity (original phases) and $x_{ng1}(t)$ just shows the trivial data of a Gaussian distributed random signal (equally distributed phases), which give no further information about non-Gaussianities. Same observation can be made for the second half of the frequency range at the respective frequency bands. Simply put, the greater values in the trispectra allow a location of non-Gaussianities related to certain frequency bands.

3.2 Fatigue analysis of a vibration system

Both non-Gaussian signals $x_{ng1}(t)$ and $x_{ng2}(t)$ where used as an excitation for a vibration system in order to determine response signals $y_{ng1}(t)$ and $y_{ng2}(t)$ (see Fig. 1). Further, these responses (also in terms of excitations) were interpreted as stress signals to be able to perform a fatigue analysis. In order to make such a fatigue analysis independent from a specific vibration system, the Fatigue Damage Spectrum (FDS) [15] is typically used. It is based on a single degree of freedom vibration system with a variable natural frequency f_o which is supposed to model an arbitrary behaviour of an unknown vibration system. It enables a comparison of equivalent fatigue loads s_{eq} of the vibration response $y(t)$ caused by different excitations $x(t)$ (see Fig. 4). The corresponding equation of motion is given in Eq. (17) (with mass m, stiffness c and damping d). These parameters

c, d and m are reduced to the damping ratio D (further exemplarily set to 3%) and the natural angular frequency ω_o.

$$\ddot{y}(t) + 2D\omega_0\dot{y}(t) + \omega_o^2 y(t) = \ddot{x}(t); \quad \text{with: } \omega_0 = \sqrt{c/m}; \quad D = \frac{d}{2m\omega_0} \tag{17}$$

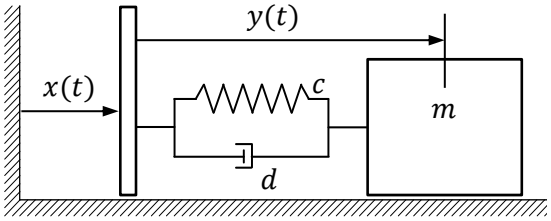

Figure 4: One dof vibration system

These response signals $y_{ng1}(t)$ and $y_{ng2}(t)$ are further used for a fatigue analysis (see Fig. 1), which means evaluating load spectra by either counting (RFC) or estimation (DK) techniques and using PM as damage accumulation theorem (exemplarily with the Miner Exponent $k = 5$ and endurance cycle number $N_{eq} = 1$) to assess equivalent fatigue loads s_{eq}. It is important to know that the RFC is a fatigue cycle counting method, not an estimation method, and hence, it is not bounded to any limitation of the distribution of $y(t)$. Hence, the RFC is typically interpreted as the reference. The described procedure is evaluated several times with different natural frequencies f_0 (here for $0 < f_0 < 600$ Hz) to make the fatigue analysis independent from an individual vibration system.

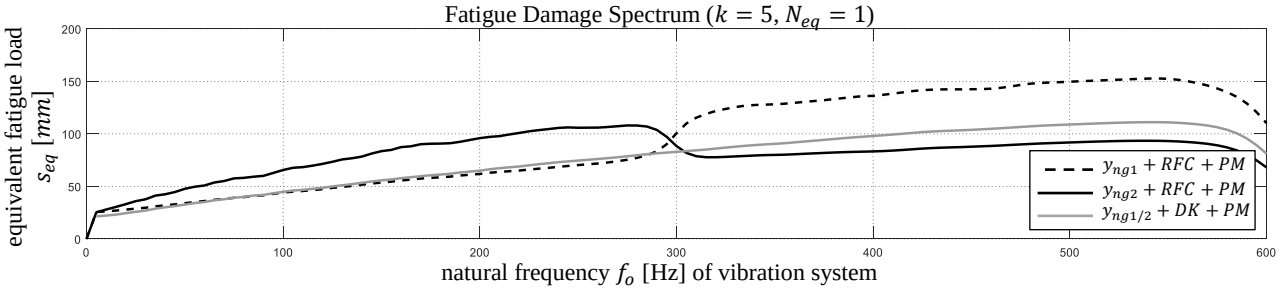

Figure 5: FDS derived from non-Gaussian vibration loads $\boldsymbol{x_{ng1}(t)}$ and $\boldsymbol{x_{ng2}(t)}$ by using RFC and DK for load spectra evaluation, with Miner Exponent $\boldsymbol{k = 5}$ and endurance cycle number $\boldsymbol{N_{eq} = 1}$

The FDS depicted above shows the fatigue analysis of a variable vibration system, when being subjected to the non-Gaussian random vibration loads $x_{ng1}(t)$ and $x_{ng2}(t)$. The fatigue analyses, which were evaluated by RFC from $y_{ng1}(t)$ and $y_{ng2}(t)$ in time domain count as a reference. Since both non-Gaussian vibration loads share the same PSD, they also produce the same PSD-based fatigue analysis using the DK estimator. It is clearly seen, that the PSD-based fatigue analysis underestimates the structures fatigue, expressed as equivalent fatigue load. Since the PSD is only depending on the magnitude of Fourier coefficients, phases have no influence. Nevertheless, phases are highly important for the characterisation of non-Gaussian signals in frequency domain. It is obvious, that the two compared non-Gaussian random vibration signals cause different fatigue loads on the vibration system depending on its natural frequency; their kurtosis values are not able to indicate that deviation. Consequently a single kurtosis value is not sufficient for a clear characterisation of non-Gaussianity. The proposed higher order spectral analysis makes these differences visible. The presented method can be applied to long time signals as they usually appear in the area of fatigue analysis and can help to avoid underestimation of fatigue loads. The results also prove that a reliable fatigue assessment has to take into account that higher order statistical moments have a distribution in the frequency range of the analysed signals.

4. Conclusion

This paper has shown that a single kurtosis parameter is insufficient for characterising the deviation of a non-Gaussian random signal to its corresponding Gaussian signal. It was pointed out that the kurtosis can be represented by central moments and hence has a distribution in frequency domain. An adequate characterisation of a non-Gaussian vibration load can be achieved by the use of higher order spectra. In this paper, the application of trispectra has helped to characterise the impact of

certain non-Gaussian vibration loads onto the fatigue load of a vibration system. In addition, since random vibration loads appear to be very long in time, a very efficient and robust method for the calculation of higher order spectra was presented. The results cannot yet serve as a complete solution to the problem of non-Gaussianity in the area of fatigue loads but they offer a new powerful analysis tool for a better understanding and precise characterisation of non-Gaussian signals. Further steps will be necessary to build reliable tools for this class of fatigue problems.

5. Acknowledgement

This work has been funded by Siemens AG and Bayerische Forschungsstiftung, project 1142/14.

REFERENCES

1 Matsuishi, M., Endo, T. Fatigue of metals subjected to varying stress. *Proceedings of the Kyushu Branch of Japan Society of Mechanics Engineering*, 37-40, Fukuoka, Japan, 1968.

2 Miner, M.A. Cumulated damage in fatigue, *Journal of Applied Mechanics*, Vol.12, Is. 3, 149-164, 1945.

3 Wannenburg, J., Heyns, P.S., Raath, A.D. Application of a fatigue equivalent static load methodology for the numerical durability assessment of heavy vehicle structures, *Intern. Journal of Fatigue*, 2009.

4 Brandt, A. Noise and vibration analysis: signal analysis and experimental procedures, John Wiley and Sons, 2011.

5 Wirsching, P.H., Paez, T.L., Ortiz, H. Random vibrations, theory and practice, New York, Wiley, 1995.

6 Clough, R.W., Penzien, J. Dynamics of structures. Computers and Structures Inc., 2004.

7 Dirlik, T. Application of computers in fatigue analysis, University of Warwick, 1985.

8 Benasciutti, D., Tovo, R. Comparison of spectral methods for fatigue analysis of broad-band Gaussian random processes, *Probabilistic Engineering Mechanics*, 2006.

9 Mršnik, M., Slavič, J., Boltežar, M. Frequency-domain methods for a vibration-fatigue-life estimation – application to real data, *International Journal of Fatigue*, 2013.

10 Braccesi, C., Cianetti, F., Lori, G., Pioli, D. The frequency domain approach in virtual fatigue estimation of non-linear systems: the problem of non-Gaussian states of stress. *Int. J. of Fatigue*, 2009.

11 Wolfsteiner, P., Breuer, W. Fatigue assessment of vibrating rail vehicle bogie components under non-Gaussian random excitations using power spectral densities. *J. of Sound and Vib.*, 2013.

12 Benasciutti, D., Tovo, R. Fatigue life assessment in non-Gaussian random loadings, *International Journal of Fatigue*, 2006.

13 Yuan, Y., Cheng, J.S. A new method for fatigue life estimation under non-Gaussian random vibration, *International Journal of Vibration and Shock*, 2014.

14 Wolfsteiner, P. Fatigue assessment of non-stationary random vibrations by using decomposition in Gaussian portions, *International Journal of Mechanical Sciences*, 2016.

15 Lalanne, C. Mechanical vibration and shock analysis, Vol. 1-5, Hoboken, John Wiley and Sons, 2009.

16 Bendat, J.S., Piersol, A.G. Engineering applications of correlation and spectral analysis, New York, John Wiley and Sons, 1980.

17 Peinelt, R.H. Analyse und Simulation nicht-Gaußscher Prozesse, Universität Innsbruck, 1992.

18 Bendat, J.S., Piersol, A.G. Random data: analysis and measurement procedures, Hoboken, John Wiley and Sons, 2010.

19 Nikias, C.L., Petropulu, A.P. Higher-order spectra analysis: a nonlinear signal processing framework, Englewood Cliffs, 1993.

20 Nikias, C.L., Mendel, J.M. Signal processing with higher-order spectra, *IEEE Signal Processing Magazine*, 1993.

21 Petropulu, A.P. Higher-order spectral analysis, *The Biomedical Engineering Handbook*, 1999.

22 Madsen, H., Holst, J. Modelling non-linear and non-stationary time series, 2007.